

High-Pressure Synthesis of 1D Low-Bandgap Polymers Embedded in Diamond-like Carbon Nanothreads

Sebastiano Romi, Samuele Fanetti,* Frederico G. Alabarse, Roberto Bini,* and Mario Santoro*



Cite This: *Chem. Mater.* 2022, 34, 2422–2428



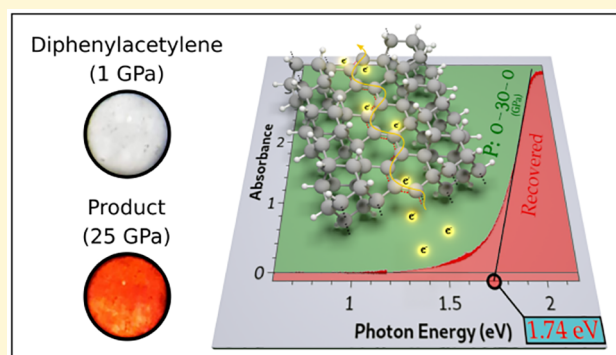
Read Online

ACCESS |

Metrics & More

Article Recommendations

ABSTRACT: The synthesis of hydrogenated carbon nanothreads at tens of GPa from aromatic systems is one of the most brilliant recent findings in high-pressure science. C-nanothreads combine the high tensile strength of diamond with the high flexibility of polymers, and many efforts are currently being undertaken to tailor some useful physicochemical properties by smartly modifying their local structure. We present the synthesis of double core diamond-like nanothreads with the two cores being bound by a conjugated C, polyacetylene-like backbone. The two cores also form a protecting sheath for the backbone. This material exhibits an optical bandgap of 1.74 eV, similar to polyacetylene; it is then very attractive as a potential organic semiconductor with simultaneous outstanding mechanical properties. The synthesis was achieved by reacting diphenylacetylene in diamond anvil cells, at 25–30 GPa and room temperature, and the materials were characterized by optical spectroscopy, synchrotron X-ray diffraction, and ab initio computer simulations.



INTRODUCTION

High-pressure methods strongly enhance the reconstruction of chemical bonds in condensed matter, thereby offering a versatile approach for the synthesis of a rich variety of exotic yet potentially useful materials. Specifically, the high-pressure synthesis of 1D hydrogenated C-nanothreads, at tens of GPa, from simple aromatic compounds, has been generating a vibrant research field through the past decade.^{1–18} In the ideal thread of this sort, carbon is entirely sp³ hybridized, resulting in an overall linear, diamond-like structure with transverse shape and size reflecting those of the starting aromatic monomer, and benzene is certainly the archetypal example in this respect.^{1–3} In principle, this unique structure merges the high tensile strength of diamond to the high flexibility of polymers. C-nanothreads pack together with no long-range order along the thread axis and 2D close-packed, pseudo-hexagonal crystalline order in the orthogonal plane. The packing exhibits a transverse spatial correlation length of several nanometers, and it may result in strongly oriented polycrystalline bundles with tens of nanometers up to a micrometer-size cross section and a total length of up to 100 μm. Although nowadays the transformation of dense small aromatic hydrocarbon systems into C-nanothreads seems to be a quite general property of this class of molecules at extreme conditions, the leading transformation mechanism may differ. For instance, in benzene, the synthesis is driven by the large uniaxial stress provided by the two opposed anvils in diamond anvil cells (DACs) or in Paris–Edinburgh cells in the absence of pressure

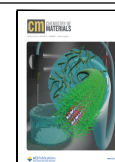
transmitting medium (PTM), and, as a consequence, the process is a mechanochemical synthesis.³ Instead, the intrinsic structural anisotropy in the starting molecular crystal has been suggested to be the relevant transformation mechanism in aniline⁵ and azobenzene,¹⁸ these ones too nonhydrostatically compressed, and the reactions are topochemical in these cases. Anyway, uniaxial stress is generally found to strongly enhance the orientation of the nanothreads along the anvil axes.

The unique mechanical properties originally foreseen for benzene-derived C-nanothreads would lead to applications of these compounds as unprecedented mechanical energy storage materials¹⁹ or heat transport materials.²⁰ The possibility to introduce additional chemical and physical features such as chromophore doping, among others, without worsening the mechanical quality, has been experimentally and computationally pursued by starting the synthesis from polycyclic, hetero-, and substituted aromatic compounds.^{4,5,8,12,15,17,21,22} In this way, it was possible to form either nanothreads with backbone carbon partially substituted by the heteroatom or nanothreads whose surface is decorated by hydrogen-replacing functional

Received: December 30, 2021

Revised: February 8, 2022

Published: February 16, 2022



groups. Now, adding electric transport properties to hydrogenated C-nanowires would be a substantial plus. On the other hand, spatially delocalized electrons are incompatible with the diamond-like structure of the threads, and, to achieve a conductive or semiconductive version of these materials, some amount of unsaturated sp^2 carbon should be included in the thread backbone. Computer simulations have been predicting such a possibility, while some cost is paid in terms of decreased strength and stiffness of the threads.²³ In this experimental work, we present an alternative approach, which preserves the full diamond-like structure of the nanowires. Here, the starting monomer is diphenylacetylene (DPhA). We expected that C coordination in the acetylene and aromatic moieties could both and somewhat independently increase by 1 at high pressures, as indicated in a previous study,²⁴ which may provide extended unsaturated carbon and extended diamond-like carbon structures, intercalated with each other. Indeed, on the basis of a combination of different methodologies, nonhydrostatic compressions in DAC up to 25–30 GPa at room temperature, IR and visible absorption spectroscopies, synchrotron X-ray diffraction (XRD), and ab initio computer simulations, we will show that the high-pressure transformation of DPhA results in double-core, diamond-like nanowires where the two parallel threads of the core are linked by a polyacetylenic and hence likely semiconductive chain. In turn, the chain is protected by the diamondoid sheath. The novel material is found to exhibit a low optical bandgap, which could join the realm of mechanically robust carbon nanowires to the broad field of organic electronics. Interestingly, related nanostructured carbon materials with mixed sp^3 – sp^2 bonding, hence potentially conductive, are also emerging from work on natural and synthetic carbon phases with graphene-like units embedded in and coherently bonded to diamond matrixes.^{25,26}

EXPERIMENTAL AND COMPUTATIONAL METHODS

Crystalline diphenylacetylene (Sigma-Aldrich, purity >98%) was ground and loaded into membrane diamond anvil cells (MDACs) equipped with Ila-type synthetic diamonds. A ruby or a gold chip was added for pressure measurements, which we performed using, respectively, the ruby fluorescence method²⁷ or the gold equation of state.²⁸ The samples were laterally contained by stainless steel gaskets with an initial sample diameter and thickness of about 150 and 50 μm , respectively. No pressure transmitting medium was used to enhance the transformation of diphenylacetylene into carbon nanowires.

Fourier transform infrared absorption (FTIR) spectra in the 500–16 000 cm^{-1} frequency range were measured using a Bruker-IFS 120 HR spectrometer equipped with blackbody broadband sources and suitably modified for experiments in diamond anvil cells, with a frequency resolution set to 1 cm^{-1} .²⁹ Absorption spectra with similar resolution, in the 12 900–17 500 cm^{-1} frequency range, were also measured using a light-emitting diode source, a single grating monochromator (Acton/SpectraPro 2500i), and a Raman grade CCD detector (Princeton Instruments Spec-10:100BR). The ruby fluorescence was excited using <1 mW of a 532 nm laser line, a low power that was found to be unable to photoinduce chemical reactions in diphenylacetylene over the entire investigated pressure range.

Angle-dispersive X-ray diffraction measurements were performed on the high-pressure diffraction beamline from the Elettra Synchrotron Facility, Xpress, using a Dectris PILATUS3 6M area detector. The incident wavelength was 0.49499 Å, and the beam diameter was about 80 μm (fwhm). The diffractometer was calibrated

using a CeO_2 powder standard, and the 2D diffraction patterns were analyzed and integrated using Dioptas.³⁰

Quantum chemistry calculations were performed using Gaussian 16³¹ to obtain the optimized structures, vibrational frequencies, and IR spectra for nanowire fragments composed of six diphenylacetylene molecular units. The calculations were based on the Density Functional Theory (DFT), adopting the Becke's three-parameter hybrid exchange functional and the Lee–Yang–Parr correlation functional (B3LYP),^{32,33} using the 6-311G(d,p) basis set. No imaginary vibrational frequencies were obtained, indicating that the optimized vacuum geometries are at the minimum of the potential surface.

RESULTS AND DISCUSSION

Optical Bandgap Measurements. Room-temperature compression of DPhA to 25–30 GPa resulted in a visually deep red material, indicating that a conjugated carbon compound is formed. For a more quantitative description of these changes, we measured the optical band gap absorption spectra of DPhA under pressure, in the IR–NIR–VIS frequency range (Figure 1). In the top panel, we report the selected spectra for a typical sample in a DAC, measured over the 0–29–0 GPa pressure cycle. An absorption edge suddenly appears upon increasing pressure above several GPa, which becomes progressively stronger and more red-shifted at higher pressures, and this behavior is only very slightly reverted along the pressure downstroke. The changes observed upon pressure increase are very likely to be driven by the irreversible increasing amount of optically absorbing reaction product and also by the reversible band gap closing of this material. The two effects are entangled, although the first one seems to largely prevail, because the formation of the bandgap absorption is only barely reversible. Anyway, what matters here the most is the bandgap absorption spectrum of the recovered material (Figure 1, bottom panel). This spectrum was measured over a more extended energy range, and it exhibits a clear inflection point at around 2.0 eV, which, through a linear fit and extrapolation procedure, led us to find a value of 1.74(5) eV for the optical bandgap energy. This value can be compared to those obtained for *trans*- and *cis*-polyacetylene, 1.4 and 1.9 eV, respectively, whose spectra are also reported in the figure after re-elaboration of literature data.³⁴ Polyacetylene (PA) is a textbook organic semiconductor, and our newly synthesized material having an intermediated bandgap energy between those of the two PA conformers can be straightforwardly classified as an organic semiconductor as well. Also, interestingly, the literature *trans*-PA exhibits a single bandgap absorption spectrum, whereas *cis*-PA shows a double bandgap, which was traced back to the presence of *trans*-PA phase impurities.³⁴ Similar to *trans*-PA and at variance with the impure *cis*-PA sample, our material shows a single bandgap absorption spectrum, which points to a single conjugated carbon conformer; this conformer, according to the bandgap value, likely belongs to the *cis*-type. Through the following chemical and structural investigation, we will show that diamond-like carbon nanowires are formed in the high-pressure reaction product of DPhA, similar to all of the other aromatic systems studied so far, and we will describe how the nanowires are connected to the polyacetylenic carbon chains.

Vibrational Spectroscopy Characterization. Vibrational spectroscopy provides direct information on the high-pressure chemical modifications. Here we focus on IR absorption spectroscopy, whereas Raman spectroscopy was

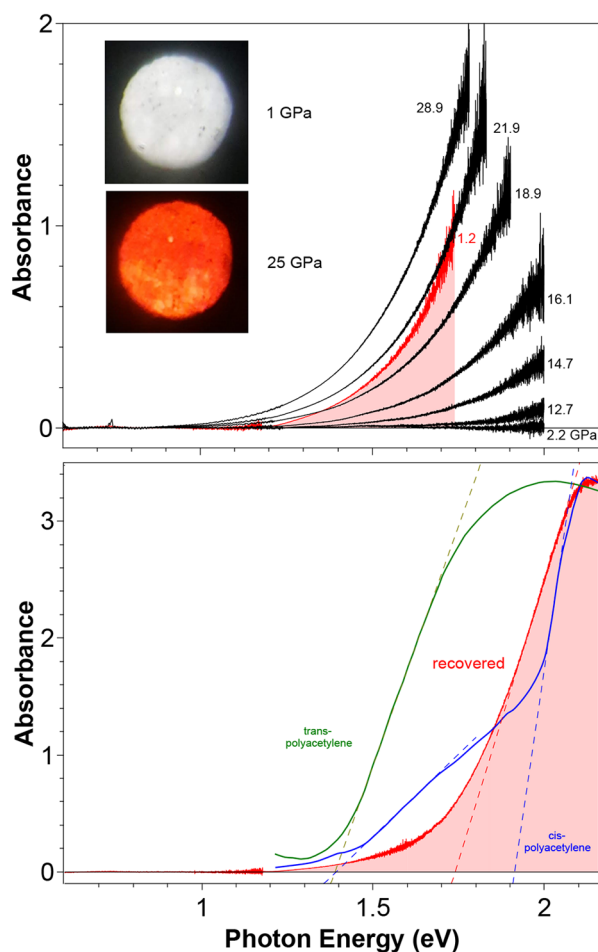


Figure 1. Optical band gap absorption spectra of compressed DPhA. Top panel: Spectra measured upon increasing (black) and decreasing (red) pressure, measured by the FTIR setup. Labeling numbers are the pressure values in GPa. Inset: Pictures of the initial, monomeric sample at 1 GPa and of the compressed sample at 25 GPa, recorded in transmitted light. Sample diameter was about 150 μm . Bottom panel: Spectrum of a transformed DPhA sample (red), recovered at ambient pressure in a free-standing gasket, measured over an extended energy range accessed by combining the FTIR and the visible absorption setup. The green and blue spectra correspond to *trans*- and *cis*-polyacetylene, respectively, and are adapted with permission from ref 34. Copyright 1982 The American Physical Society. The two band gap structure for *cis*-polyacetylene is due to a *trans*-phase impurity. The intersection of the dashed lines with the horizontal, null line identifies the band gap values.

prevented by a strong luminescence background sharply increasing with the growing amount of reacted material. Also, we aimed to avoid spurious, laser-induced photochemical effects. In Figure 2, top panel, we report on selected IR spectra measured on a DPhA sample upon increasing and subsequently decreasing pressure, in the 0–30–0 GPa pressure range. The initial sharp molecular peaks, several of which saturate the absorption, progressively decrease in intensity over the upstroke run up to 16 GPa, and then much more sharply above this pressure. At 24.1 and 30.0 GPa, only the strongest molecular peaks can be observed with their intensity being reduced by at least 1 order of magnitude, suggesting that a significant amount of DPhA was transformed. In parallel, new distinct, broad, and weak bands appeared, which we easily ascribe to the DPhA derived nonmolecular material produced.

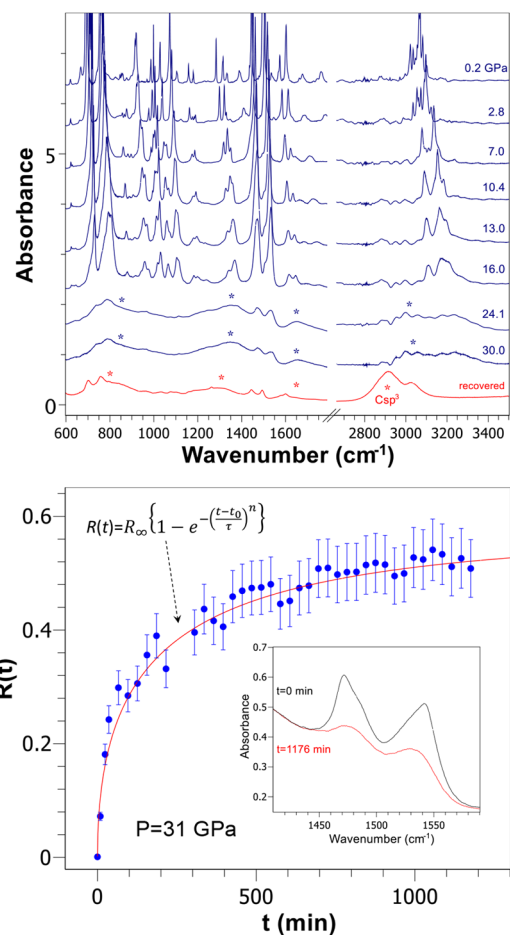


Figure 2. IR absorption spectra and transformation kinetics of DPhA under pressure. Top panel: Selected IR spectra of DPhA along a typical compression (dark blue lines)/decompression (red line) run. Labeling numbers are the pressure values in GPa. *: Labels for broad bands assigned to the extended reaction product. Particularly, the product band at 2910 cm^{-1} is ascribed to the C–H stretching modes for C in sp^3 hybridization. Interference fringes affect the high-pressure spectra at $2800\text{--}3300 \text{ cm}^{-1}$, especially above 10 GPa. The spectra have been vertically split for the sake of clarity. Bottom panel: Fraction of reacted monomer versus time, at $P = 31$ GPa. Blue \bullet : Experimental data. Red line: Avrami model fitted to the experimental data (see text) with parameters $R_{\infty} = 0.57$, $\tau = 204 \text{ min}$, $t_0 = 5.5 \text{ min}$, and $n = 0.51$. Inset: Molecular IR peaks at the initial and final time, used for evaluating the quantity $R(t)$.

In the recovered sample, the nonmolecular bands are centered at about 800 , 1300 , 1640 , and 2910 cm^{-1} , respectively, and their large bandwidth points to some degree of disorder. The band at 2910 cm^{-1} corresponds to C–H stretching modes for C in sp^3 hybridization, and, as a consequence, it is the clear signature of a novel extended material having hydrogenated sp^3 C, similarly to C-nanotreads, coexisting with conjugated C species found with the optical bandgap measurements. Weak and broadened molecular peaks are also retained in the transformed sample, which points to some amount of residual highly strained molecular materials, likely encapsulated in the nonmolecular solid. The integrated intensity ratio between the partially resolved $\text{C}(\text{sp}^3)\text{--H}$ and $\text{C}(\text{sp}^2)\text{--H}$ stretching bands centered at 2910 and 3030 cm^{-1} , respectively, leads one to estimate the $\text{C}(\text{sp}^3)/\text{C}(\text{sp}^2)$ concentration ratio for the hydrogenated carbon species, through a heuristic procedure

described elsewhere.³⁵ In short, we find $C(\text{sp}^3)/C(\text{sp}^2) = 2.2$ for the recovered material.

In addition to pressure variations, the IR spectra also change as a function of time along the chemical transformation, albeit to a lesser extent. The investigation of kinetic effects adds to the chemical and structural description of the product. In Figure 2, bottom panel, we report the time behavior of the fraction $R(t)$ of the reacted monomer, at 31 GPa, which is a pressure well above the reaction threshold. $R(t)$ is defined as $R(t) = 1 - A(t)/A(0)$, where $A(t)$ and $A(0)$ are the total integrated intensities of selected IR molecular peaks at time t and at the initial observation time, respectively. We focused on two molecular peaks at about 1475 and 1530 cm^{-1} , still decently observable at these pressures. The experimental quantity $R(t)$ is a monotonic increasing function of time, and we successfully fitted this quantity to an Avrami kinetic curve, which is a suitable model for diffusion-controlled solid-state reactions.³⁶ The Avrami model relies on four parameters: the asymptotic amplitude, R_∞ , the rise time constant, τ , the initial time, t_0 , and the parameter n related to the dimensionality of the process. In our case, we find $\tau = 204$ min and $R_\infty = 0.57$. Anyway, what matters here the most for giving a clue to the structure of the reaction product of DPhA is the parameter n , which results as equal to 0.51; this value, as any value smaller than 1, immediately points to a 1D growth process of the product as expected for the formation of nanothreads.

XRD Characterization of Double-Core C-Nanothreads. Direct structural information on the transformation is provided by powder XRD. In Figure 3, we report the selected XRD patterns measured over a compression/decompression run, at 0–27–0 GPa. The sharp Bragg peaks of DPhA observed at ambient pressure broaden and shift to a higher exchanged Q moment upon increasing pressure. At 9.8 GPa, a new weak peak is observed at around 0.62 \AA^{-1} , signaling the transition to a new phase, which we suggest to be molecular, on the basis of IR spectroscopy. The new phase appears to be the seed for the transformation to the nonmolecular product, occurring at higher pressures, similar to what has been recently observed in an analogous system: azobenzene.¹⁸ Upon increasing pressure to 27.0 GPa, all diffraction peaks vanish except those at about 0.6 and 1.2 \AA^{-1} , which become very weak. Upon subsequently decreasing pressure, these peaks intensify, and, in the recovered product, we found them to be positioned on average, over a set of four distinct recovered samples, at $0.566(7) \text{ \AA}^{-1}$ (d -spacing = $11.1(1) \text{ \AA}$) and $1.16(1) \text{ \AA}^{-1}$ (d -spacing = $5.41(5) \text{ \AA}$), respectively. This behavior shows that a substantial amount of disorder is introduced in the system along the pressure run, to yield a partially crystalline sample once back at ambient pressure. Importantly, the peak at higher Q is close to the strong (100) peak of benzene-derived C-nanothreads packing together in a pseudo-hexagonal 2D structure, with an interthread distance of 6.47 \AA .^{1,3} The simultaneous presence of a peak at nearly one-half of the Q value can be easily interpreted as the evidence of double-core C-nanothreads packed in a pseudo-hexagonal structure, similar to the recently reported case of azobenzene-derived C-nanothreads.¹⁶ In addition to these two diffraction peaks, we observe a much broader and diffuse peak at around 1.35 \AA^{-1} . This peak suggests the presence of a more disordered form, likely the residual unreacted and highly strained DPhA, also observed in the IR spectra, coexisting with the nanothreads. Following the interpretation of the azobenzene-derived C-nanothreads, we

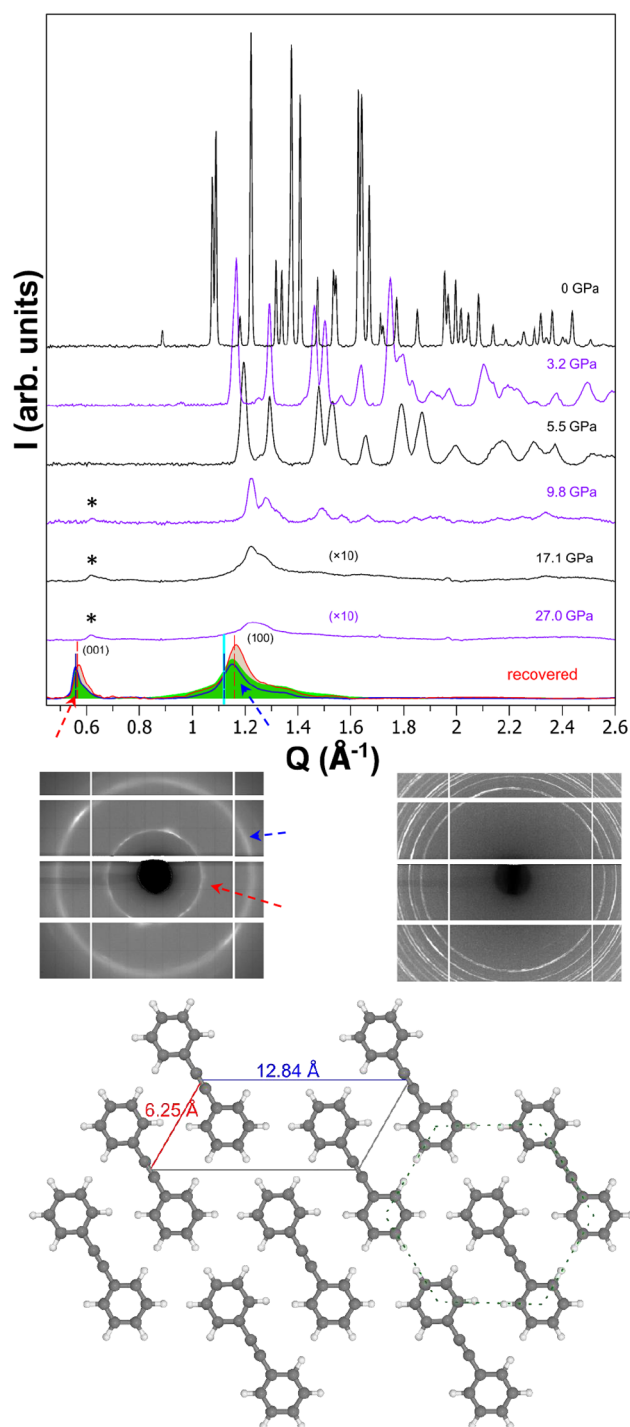


Figure 3. Powder XRD patterns of DPhA under pressure and the structure of the recovered reaction product. Top panel: Selected, azimuthally integrated patterns measured upon increasing pressure (black and violet), and recovered at ambient pressure (red, green, and blue, for three distinct samples). *: New peak observed above 9.8 GPa (see text). Vertical lines: Q position for the peaks of DPhA-derived (red), benzene-derived (cyan),^{1,3} and azobenzene-derived (dark blue) C-nanothreads.¹⁶ Intermediate panels: Ambient pressure 2D XRD patterns for the recovered (left) and the initial (right) samples. Bottom panel: Schematic, crystalline 2D arrangement of the nanothreads, represented by DPhA proxies, in the plane orthogonal to the thread axis. The monoclinic cell and the corresponding lattice parameters are evidenced as well as the hexagonal arrangement of the threads (dashed line).

describe the present nanothread structure by means of a monoclinic primitive cell ($a = 6.25 \text{ \AA}$, $c = 12.8 \text{ \AA}$, $\beta = 120^\circ$) reported in Figure 3, where the double-core nanothreads are represented by DPhA proxies. This structure well accounts for the two observed diffraction peaks at 0.566 and 1.16 \AA^{-1} , which we can now index as (001) and (100), respectively. The full width at half-maximum (fwhm) of the peaks then provides an estimation of crystallinity. We estimate the orthogonal spatial correlation length l ($l \approx 2\pi/\text{fwhm}$) for the crystalline packing of the nanothreads to be at minimum 60 and 300 \AA for the [100] and the [001] directions, respectively. The correlation length for the [100] direction is in good agreement with the value found in the benzene-derived nanothreads.¹ These l values need to be considered as a low limit estimation of the true values, which could rather be masked by strain effects. In fact, the observed fwhm is likely to be increased by the potential strain-related statistical distribution of d -spacing values over the relatively large ($80 \mu\text{m}$) X-ray beam-spot. A close look at the 2D XRD patterns (Figure 3) then reveals an enhanced texture in the recovered sample with respect to the almost randomly oriented starting powder material. This is an effect of the uniaxial stress, which enhances the orientation of the nanothreads along the axis of the applied pressure load. However, our recovered sample is far from being single-crystal-like, as was observed in other aromatic systems-derived C-nanothreads, indicating that the uniaxial stress is likely opposed by the intrinsic anisotropy of the starting DPhA crystal. The accurate and quantitative characterization of the interplay between this anisotropy and the uniaxial stress in driving the reaction mechanism from the monomer to the nanothreads would mandatorily involve single-crystal XRD data, provided that sufficient single-crystal quality could be retained along the entire reaction path. This task is definitely beyond the scope of the present work. It is also worth noting that the present XRD-based identification of carbon nanothreads parallels the information obtained by optical spectroscopy, indicating that the high-pressure reaction of DPhA followed a 1D growth and resulted in the formation of a substantial amount of carbon in sp^3 hybridization.

Ab Initio Computer Simulations of the C-Nanothread Structures. Additional structural information on our double-core nanothreads can be obtained by Density Functional Theory (DFT) methods. While each single core likely results from the self-assembling of phenyl rings into polymeric structures with C entirely in sp^3 hybridization, similar to benzene, the fate of the carbon atoms from the acetylene moieties needs to be clarified. It is reasonable to expect that these atoms are the “glue” that binds together two polymers of this sort. Following the recent findings on azobenzene-derived double-core nanothreads,¹⁶ we focused our analysis on two distinct diamond-like polymers: tube (3,0) and polymer 1. We considered the possibility to link these polymers by either a C conjugated polyacetylene-like backbone, obtained from the polymerization of the acetylene moieties, or by just the unreacted moieties, in a ladder-like fashion. We then performed DFT structural optimizations over a total of four distinct nanothreads fragments composed of six molecular units (Figure 4): (i) conjugated C-tube (3,0), (ii) conjugated C-polymer 1, (iii) triple CC bond-tube (3,0), and (iv) triple CC bond-polymer 1. After the optimization, no imaginary vibrational frequencies were obtained, thereby showing that all of the considered structures are locally stable. Incidentally we note that, due to the geometrical constraints given by the

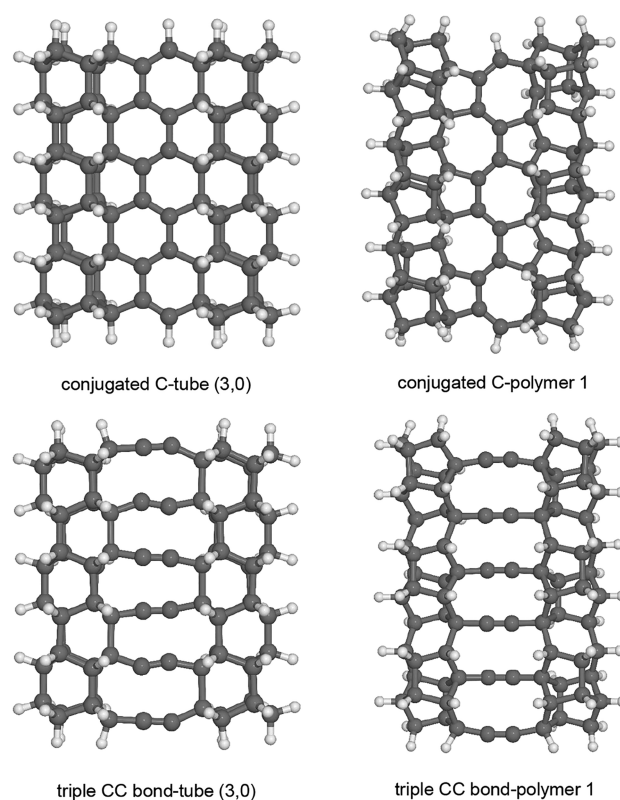


Figure 4. DFT-optimized structures of nanothread fragments composed of six DPhA units (see text). Top (lower) panels: Two diamond-like nanothreads are linked together by conjugated C backbones (ladders of CC triple bonds).

double core nanothread structure, the *cis*-type polyacetylene-like backbone is the only possible polyacetylenic conformer that can act as a linker between the cores. In fact, it is not possible to fit a *trans*-type polyacetylene-like chain within the two threads without the disruption of the double core structure itself. In Figure 5, we report the comparison between the IR spectra of the four simulated structures, together with the spectrum of a DFT simulated single molecule, and the experimental spectrum of a typical recovered sample, obtained after compression of DPhA to 30 GPa. As was observed above, the spectrum of the recovered sample exhibits several broad bands for the reaction product and a number of much sharper peaks originating from highly strained molecular remnants. While all of the simulated structures reproduce the broad band at around 1300 cm^{-1} , only conjugated C-tube (3,0) and conjugated C-polymer 1 reproduce the product bands in the $1600\text{--}1700 \text{ cm}^{-1}$ frequency range. Also, among all of the structures, conjugated C-tube (3,0) better agrees with the observed broad band at around 800 cm^{-1} . In short, this comparison supports double-core nanothreads linked by *cis*-type polyacetylene-like backbones as a major component of the recovered sample. These structures are also supported by the observed optical bandgap absorption spectrum (Figure 1), which exhibits a bandgap of intermediate value between those of *trans*- and *cis*-type polyacetylene, yet somewhat closer to that of the *cis*-type conformer.

CONCLUSIONS

The compression of diphenylacetylene to tens of GPa led us to synthesize a nonmolecular material whose optical bandgap at

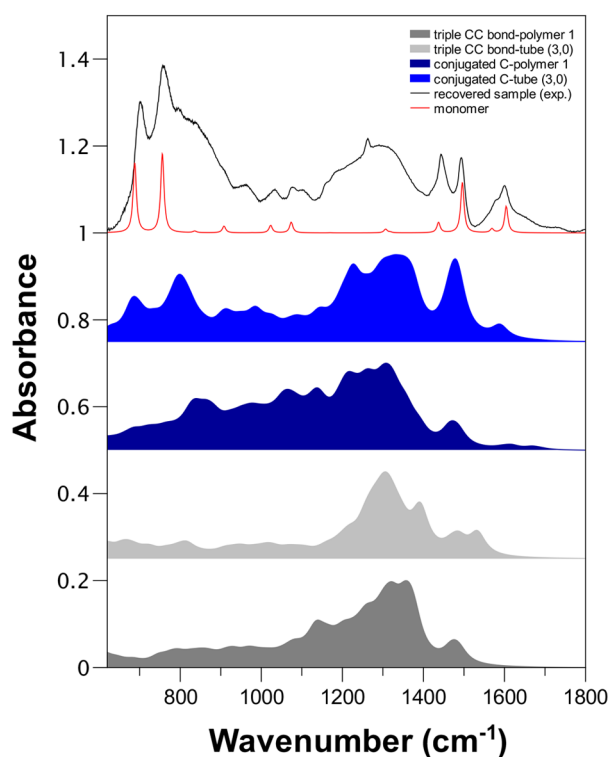


Figure 5. Comparison between the experimental IR spectrum of a recovered sample (black) and DFT calculated IR spectra of four distinct DPhA-derived double-core nanothreads (blue and gray). Blue, conjugated C-tube (3,0); dark blue, conjugated C-polymer 1; light gray, triple CC bond-tube (3,0); gray, triple CC bond-polymer 1. Red spectrum: DFT calculated IR spectrum of a DPhA molecule. Frequency line widths in the DFT spectra have been set to highlight the comparison to the experimental peaks. The spectra have been vertically offset for the sake of clarity.

ambient pressure is equal to 1.74 eV, a typical value for organic semiconductors. Our combined optical spectroscopy, XRD, and DFT investigation coherently shows that this material is made of 1D diamond-like, double-core hydrogenated C-nanothreads packed together with 2D pseudo-hexagonal order in the orthogonal plane and spatial correlation lengths in this plane of at least 60–300 Å. In this respect, our material is similar to the polymeric high-pressure reaction product of many other simple aromatic systems. However, the two threads of the double-core are linked by conjugated C, polyacetylene-like backbones, which makes the material an organic semiconductor and hence a unique case among the class of known C-nanothreads. Our novel material is then expected to combine the excellent mechanical properties of diamond-like nanothreads with the transport properties of a text-book polymeric semiconductor, polyacetylene, a result that significantly adds to the rich variety of potential applications of C-nanothreads. Finally, the encapsulated polyacetylene-like chains are more physically and chemically robust than is pure polyacetylene. Indeed, our recovered samples were found to be stable over weeks, with no signs of reaction with atmospheric moisture (no OH stretching peaks in the IR spectra), which in turn easily occurs in polyacetylene.

AUTHOR INFORMATION

Corresponding Authors

Samuele Fanetti – European Laboratory for Nonlinear Spectroscopy (LENS), Sesto Fiorentino (FI) 50019, Italy; Consiglio Nazionale delle Ricerche - Istituto di Chimica dei Composti OrganoMetallici, Sesto Fiorentino (FI) 50019, Italy; orcid.org/0000-0002-5688-6272; Email: fanetti@lens.unifi.it

Roberto Bini – European Laboratory for Nonlinear Spectroscopy (LENS), Sesto Fiorentino (FI) 50019, Italy; Consiglio Nazionale delle Ricerche - Istituto di Chimica dei Composti OrganoMetallici, Sesto Fiorentino (FI) 50019, Italy; Dipartimento di Chimica “Ugo Schiff”, Università di Firenze, Sesto Fiorentino (FI) 50019, Italy; orcid.org/0000-0002-6746-696X; Email: roberto.bini@unifi.it

Mario Santoro – European Laboratory for Nonlinear Spectroscopy (LENS), Sesto Fiorentino (FI) 50019, Italy; Consiglio Nazionale delle Ricerche - Istituto Nazionale di Ottica, Sesto Fiorentino (FI) 50019, Italy; orcid.org/0000-0001-5693-4636; Email: santoro@lens.unifi.it

Authors

Sebastiano Romi – European Laboratory for Nonlinear Spectroscopy (LENS), Sesto Fiorentino (FI) 50019, Italy; orcid.org/0000-0002-9553-7788

Frederico G. Alabarse – Elettra Sincrotrone Trieste S.C.p.A., Basovizza (TS) 34149, Italy; orcid.org/0000-0002-7375-3666

Complete contact information is available at:

<https://pubs.acs.org/10.1021/acs.chemmater.1c04453>

Notes

The authors declare no competing financial interest.

ACKNOWLEDGMENTS

We thank the European Laboratory for Nonlinear Spectroscopy (LENS) for hosting part of this research and the Fondazione Cassa di Risparmio di Firenze for the strong support. We acknowledge Elettra Sincrotrone Trieste for providing access to the XPRESS beamline and for financial support under proposal numbers 20200162 and 20205110.

REFERENCES

- (1) Fitzgibbons, T. C.; Guthrie, M.; Xu, E.; Crespi, V. H.; Davidowski, S. K.; Cody, G. D.; Alem, N.; Badding, J. V. Benzene-derived carbon nanothreads. *Nat. Mater.* **2015**, *14*, 43–47.
- (2) Chen, B.; Hoffmann, R.; Ashcroft, N. W.; Badding, J.; Xu, E.; Crespi, V. Linearly Polymerized Benzene Arrays As Intermediates, Tracing Pathways to Carbon Nanothreads. *J. Am. Chem. Soc.* **2015**, *137*, 14373–14386.
- (3) Li, X.; Baldini, M.; Wang, T.; Chen, B.; Xu, E.-s.; Vermilyea, B.; Crespi, V. H.; Hoffmann, R.; Molaison, J. J.; Tulk, C. A.; Guthrie, M.; Sinogeikin, S.; Badding, J. V. Mechanochemical Synthesis of Carbon Nanowire Single Crystals. *J. Am. Chem. Soc.* **2017**, *139*, 16343–16349.
- (4) Nobrega, M. M.; Teixeira-Neto, E.; Cairns, A. B.; Temperini, M. L. A.; Bini, R. One-dimensional diamondoid polyaniline-like nanothreads from compressed crystal aniline. *Chemical Science* **2018**, *9*, 254–260.
- (5) Fanetti, S.; Nobrega, M. M.; Teixeira-Neto, E.; Temperini, M. L. A.; Bini, R. Effect of Structural Anisotropy in High-Pressure Reaction of Aniline. *J. Phys. Chem. C* **2018**, *122*, 29158–29164.
- (6) Duan, P.; Li, X.; Wang, T.; Chen, B.; Juhl, S.; Koeplinger, D.; Crespi, V.; Badding, J.; Schmidt-Rohr, K. The Chemical Structure of

Carbon Nanotubes Analyzed by Advanced Solid-State NMR. *J. Am. Chem. Soc.* **2018**, *140*, 7658–7666.

(7) Wang, T.; Duan, P.; Xu, E.-S.; Vermilyea, B.; Chen, B.; Li, X.; Badding, J.; Schmidt-Rohr, K.; Crespi, V. Constraining Carbon Nanotube Structures by Experimental and Calculated Nuclear Magnetic Resonance Spectra. *Nano Lett.* **2018**, *18*, 4934–4942.

(8) Li, X.; Wang, T.; Duan, P.; Baldini, M.; Huang, H.-T.; Chen, B.; Juhl, S. J.; Koeplinger, D.; Crespi, V. H.; Schmidt-Rohr, K.; Hoffmann, R.; Alem, N.; Guthrie, M.; Zhang, X.; Badding, J. V. Carbon Nitride Nanotube Crystals Derived from Pyridine. *J. Am. Chem. Soc.* **2018**, *140*, 4969–4972.

(9) Juhl, S.; Wang, T.; Vermilyea, B.; Li, X.; Crespi, V.; Badding, J.; Alem, N. Local Structure and Bonding of Carbon Nanotubes Probed by High-Resolution Transmission Electron Microscopy. *J. Am. Chem. Soc.* **2019**, *141*, 6937–6945.

(10) Ward, M. D.; Tang, W. S.; Zhu, L.; Popov, D.; Cody, G. D.; Strobel, T. A. Controlled Single-Crystalline Polymerization of C₁₀H₈·C₁₀F₈ under Pressure. *Macromolecules* **2019**, *52*, 7557–7563.

(11) Friedrich, A.; Collings, I. E.; Dziubek, K. F.; Fanetti, S.; Radacki, K.; Ruiz-Fuertes, J.; Pellicer-Porres, J.; Hanfland, M.; Sieh, D.; Bini, R.; Clark, S. J.; Marder, T. B. Pressure-Induced Polymerization of Polycyclic Arene-Perfluoroarene Cocrystals: Single Crystal X-ray Diffraction Studies, Reaction Kinetics, and Design of Columnar Hydrofluorocarbons. *J. Am. Chem. Soc.* **2020**, *142*, 18907–18923.

(12) Biswas, A.; Ward, M. D.; Wang, T.; Zhu, L.; Huang, H.-T.; Badding, J. V.; Crespi, V. H.; Strobel, T. A. Evidence for Orientational Order in Nanotubes Derived from Thiophene. *J. Phys. Chem. Lett.* **2019**, *10*, 7164–7171.

(13) Gerthoffer, M. C.; Wu, S.; Chen, B.; Wang, T.; Huss, S.; Oburn, S. M.; Crespi, V. H.; Badding, J. V.; Elacqua, E. ‘Sacrificial’ supramolecular assembly and pressure-induced polymerization: toward sequence-defined functionalized nanotubes. *Chem. Sci.* **2020**, *11*, 11419–11424.

(14) Tang, W. S.; Strobel, T. A. Evidence for Functionalized Carbon Nanotubes from π -Stacked, para-Disubstituted Benzenes. *J. Phys. Chem. C* **2020**, *124*, 25062–25070.

(15) Fanetti, S.; Santoro, M.; Alabarse, F.; Enrico, B.; Bini, R. Modulating the H-bond strength by varying the temperature for the high pressure synthesis of nitrogen rich carbon nanotubes. *Nanoscale* **2020**, *12*, 5233–5242.

(16) Romi, S.; Fanetti, S.; Alabarse, F.; Mio, A. M.; Bini, R. Synthesis of double core chromophore-functionalized nanotubes by compressing azobenzene in a Diamond Anvil Cell. *Chemical Science* **2021**, *12*, 7048–7057.

(17) Huss, S.; Wu, S.; Chen, B.; Wang, T.; Gerthoffer, M. C.; Ryan, D. J.; Smith, S. E.; Crespi, V. H.; Badding, J. V.; Elacqua, E. Scalable Synthesis of Crystalline One-Dimensional Carbon Nanotubes through Modest-Pressure Polymerization of Furan. *ACS Nano* **2021**, *15*, 4134–4143.

(18) Romi, S.; Fanetti, S.; Alabarse, F.; Bini, R. Structure-Reactivity Relationship in the High-Pressure Formation of Double-Core Carbon Nanotubes from Azobenzene Crystal. *J. Phys. Chem. C* **2021**, *125*, 17174–17182.

(19) Zhan, H.; Zhang, G.; Bell, J. M.; Tan, V. B. C.; Gu, Y. High density mechanical energy storage with carbon nanotube bundle. *Nat. Commun.* **2020**, *11*, 1.

(20) Zhan, H.; Zhang, G.; Zhuang, X.; Timon, R.; Gu, Y. Low interfacial thermal resistance between crossed ultra-thin carbon nanotubes. *Carbon* **2020**, *165*, 216–224.

(21) Demingos, P. G.; Muniz, A. R. Carbon nanotubes from polycyclic aromatic hydrocarbon molecules. *Carbon* **2018**, *140*, 644–652.

(22) Silveira, J. F. R. V.; Muniz, A. R. Functionalized diamond nanotubes from benzene derivatives. *Phys. Chem. Chem. Phys.* **2017**, *19*, 7132–7137.

(23) Demingos, P.; Muniz, A. Electronic and Mechanical Properties of Partially Saturated Carbon and Carbon Nitride Nanotubes. *J. Phys. Chem. C* **2019**, *123*, 3886–3891.

(24) Ceppatelli, M.; Fontana, L.; Citroni, M. The high pressure reactivity of substituted acetylenes: A vibrational study on diphenylacetylene. *Phase Transitions* **2007**, *80*, 1085–1101.

(25) Németh, P.; McColl, K.; Garvie, L.; Salzmann, C.; Murri, M.; McMillan, P. Complex nanostructures in diamond. *Nat. Mater.* **2020**, *19*, 1126–1131.

(26) Németh, P.; McColl, K.; Garvie, L.; Salzmann, C.; Pickard, C.; Corà, F.; Smith, R.; Mezouar, M.; Howard, C.; McMillan, P. Diaphite-structured nanodiamonds with six- and twelve-fold symmetries. *Diamond Relat. Mater.* **2021**, *119*, 108573.

(27) Mao, H.; Bell, P.; Shaner, J.; Steinberg, D. Specific volume measurements of Cu, Mo, Pd, and Ag and calibration of the ruby R1 fluorescence pressure gauge from 0.06 to 1 Mbar. *J. Appl. Phys.* **1978**, *49*, 3276–3283.

(28) Heinz, D. L.; Jeanloz, R. The equation of state of the gold calibration standard. *J. Appl. Phys.* **1984**, *55*, 885–893.

(29) Bini, R.; Ballerini, R.; Pratesi, G.; Jodl, H. J. Experimental setup for Fourier transform infrared spectroscopy studies in condensed matter at high pressure and low temperatures. *Rev. Sci. Instrum.* **1997**, *68*, 3154–3160.

(30) Prescher, C.; Prakapenka, V. B. DIOPTAS: a program for reduction of two-dimensional X-ray diffraction data and data exploration. *High Pressure Research* **2015**, *35*, 223–230.

(31) Frisch, M. J.; et al. *Gaussian 16*, revision C.01; Gaussian, Inc.: Wallingford, CT, 2016.

(32) Becke, A. A new mixing of Hartree-Fock and local density-functional theories. *J. Chem. Phys.* **1993**, *98*, 1372–1377.

(33) Lee, C.; Yang, W.; Parr, R. Development of the Colle-Salvetti correlation-energy formula into a functional of the electron density. *Phys. Rev. B* **1988**, *37*, 785–789.

(34) Moses, D.; Feldblum, A.; Ehrenfreund, E.; Heeger, A.; Chung, T.-C.; MacDiarmid, A. Pressure dependence of the photoabsorption of polyacetylene. *Phys. Rev. B* **1982**, *26*, 3361–3369.

(35) Ciabini, L.; Santoro, M.; Bini, R.; Schettino, V. High pressure reactivity of solid benzene probed by infrared spectroscopy. *J. Chem. Phys.* **2002**, *116*, 2928–2935.

(36) Hulbert, S. F. Models for Solid-State Reactions in Powdered Compacts: A Review. *J. Br. Ceram. Soc.* **1969**, *6*, 11–20.